Journal of Neurochemistry

JOURNAL OF NEUROCHEMISTRY | 2015 | 132 | 642–656 doi: 10.1111/jnc.13027

ORIGINAL ARTICLE

Rhythmic control of mRNA stability modulates circadian amplitude of mouse *Period3* mRNA

Sung-Hoon Kim,*,[1] Kyung-Ha Lee,†,[2] Do-Yeon Kim,‡,[3] Eunyee Kwak,‡,[4] Seunghwan Kim§ and Kyong-Tai Kim†

*School of Interdisciplinary Bioscience and Bioengineering, Pohang University of Science and Technology, Pohang, Gyeongbuk, Korea

†Department of Life Sciences, Division of Integrative Biosciences and Biotechnology, Pohang University of Science and Technology, Pohang, Gyeongbuk, Korea

‡Department of Life Sciences, Pohang University of Science and Technology, Pohang, Gyeongbuk, Korea

§Asia Pacific Center for Theoretical Physics, National Core Research Center for Systems Biodynamics, Department of Physics, Pohang University of Science and Technology, Pohang, Gyeongbuk, Korea

Abstract

The daily oscillations observed in most living organisms are endogenously generated with a period of 24 h, and the underlying structure of periodic oscillation is an autoregulatory transcription-translation feedback loop. The mechanisms of untranslated region (UTR)-mediated post-transcriptional regulation (e.g., mRNA degradation and internal ribosomal entry site (IRES)-mediated translation) have been suggested to fine-tune the expression of clock genes. Mouse *Period3* (m*Per3*) is one of the paralogs of *P*eriod gene and its function is important in peripheral clocks and sleep physiology. m*Per3* mRNA displays a circadian oscillation as well as a circadian phase-dependent stability, while the stability regulators still remain unknown. In this study, we identify three proteins – heterogeneous nuclear ribonucleoprotein (hnRNP) K, polypyrimidine tract-binding protein (PTB), and hnRNP D – that bind to m*Per3* mRNA 3′-UTR. We show that hnRNP K is a stabilizer that increases the amplitude of circadian m*Per3* mRNA oscillation and hnRNP D is a destabilizer that decreases it, while PTB exhibits no effect on m*Per3* mRNA expression. Our experiments describe their cytoplasmic roles for the mRNA stability regulation and the circadian amplitude formation. Moreover, our mathematical model suggests a mechanism through which post-transcriptional mRNA stability modulation provides not only the flexibility of oscillation amplitude, but also the robustness of the period and the phase for circadian m*Per3* expression.

Keywords: circadian rhythm, post-transcriptional regulation, period, untranslated region, mathematical model.

J. Neurochem. (2015) **132**, 642–656.

Received August 26, 2014; revised manuscript received December 15, 2014; accepted December 19, 2014.

Address correspondence and reprint requests to Dr Kyong-Tai Kim, Department of Life Sciences, Division of Integrative Biosciences and Biotechnology, Pohang University of Science and Technology, 77 Cheongam-Ro, Nam-Gu, Pohang, Gyeongbuk 790-784, Korea. E-mail: ktk@postech.ac.kr; Dr Seunghwan Kim, Asia Pacific Center for Theoretical Physics, National Core Research Center for Systems Biodynamics, Department of Physics, Pohang University of Science and Technology, 77 Cheongam-Ro, Nam-Gu, Pohang, Gyeongbuk 790-784, Korea. E-mail: swan@postech.ac.kr

Present Addresses: [1]Division of Integrative Biosciences and Biotechnology, Pohang University of Science and Technology, Pohang, Gyeongbuk, Korea.

[2]St. Jude Children's Research Hospital, Memphis, TN 38105-3678, USA.

[3]Department of Pathology and Laboratory Medicine, Weill Cornell Medical College, New York, NY 10065, USA.

[4]Earlogic Auditory Research Institute, Seoul, Korea.

Abbreviations used: Act.D, actinomycin D; BrU, bromouridine; Dex., dexamethasone; DSPS, delayed sleep phase syndrome; DTT, dithiothreitol; ECL, enhanced chemiluminescence; GAPDH, glyceraldehyde-3-phosphate dehydrogenase; GST, glutathione *S*-transferase; GTPBP1, guanosine triphosphate-binding protein1; hnRNP, heterogeneous nuclear ribonucleoprotein; IPTG, isopropyl-1-thio-β-D-galactopyranoside; IRES, internal ribosome entry site; ITAF, IRES trans-acting factor; NAT, serotonin *N*-acetyltransferase; NMD, nonsense-mediated decay; PMSF, phenylmethylsulfonyl fluoride; PTB, polypyrimidine tract-binding protein; RHT, retinohypothalamic tract; RNA-IP, RNA immunoprecipitation; RPL32, ribosomal protein L32; RT, reverse-transcription; SDS-PAGE, sodium dodecyl sulfate-polyacrylamide gel electrophoresis; TBP, TATA-box-binding protein; UTR, untranslated region.

A wide range of living organisms from bacteria to humans have the endogenous clock, which governs most of the physiological processes and is necessary for efficient energy metabolism (Reppert and Weaver 2002; Bass and Takahashi 2010; Albrecht 2012). Since the period of the clock is about the length of a day (24 h), it is called a circadian clock. This regular rhythmicity is well known to be an endogenous and self-sustained oscillation. The fundamental molecular structure of biological clocks is a negative feedback loop, and several studies have been performed at transcriptional and post-translational levels to elucidate its function. In mammals, BMAL1 and CLOCK form a heterodimer and induce the synthesis of transcriptional repressor mRNAs that have E-boxes in the promoters of their genes, such as *Period (Per)*, *Cryptochrome (Cry)*, and *Rev-erb* α (Gekakis *et al.* 1998; Jin *et al.* 1999; Kume *et al.* 1999; Preitner *et al.* 2002). The repressor proteins PER and CRY form a heterodimer and repress the activity of BMAL1/CLOCK (Sangoram *et al.* 1998; Griffin *et al.* 1999), and REV-ERB α represses *Bmal1* transcription (Ueda *et al.* 2002; Guillaumond *et al.* 2005). Moreover, several post-translational regulators, such as casein kinase 1 δ/ε (Akashi *et al.* 2002; Lee *et al.* 2009), protein phosphatase 1 (Lee *et al.* 2011a; Schmutz *et al.* 2011), sirtuin 1 (SIRT1) (Asher *et al.* 2008; Nakahata *et al.* 2008), F-box protein β-transducin repeat-containing protein (Shirogane *et al.* 2005; Ohsaki *et al.* 2008), F-box/LRR-repeat protein 3 (FBXL3) (Busina *et al.* 2007; Siepka *et al.* 2007), and FBXL21 (Dardente *et al.* 2008; Hirano *et al.* 2013; Yoo *et al.* 2013) have been identified for their roles in the regulation of clock proteins and alterations of behavior.

Besides transcriptional and post-translational regulation, recent studies in a genome-wide scale reveal that other types of gene regulation may have roles in the rhythmic expression of clock genes (Koike *et al.* 2012; Menet *et al.* 2012; Morf *et al.* 2012). These include mRNA polyadenylation (Kojima *et al.* 2012), RNA-methylation-dependent RNA processing (Sanchez *et al.* 2010), and mRNA untranslated region (UTR)-mediated post-transcriptional regulation, such as mRNA degradation via the 3′-UTR, internal ribosomal entry site (IRES)-mediated translation via the 5′-UTR, and 3′-UTR-mediated translational regulation (Kojima *et al.* 2007). Several destabilizer proteins for clock gene mRNAs have been identified. These proteins are thought to accelerate the degradation of clock mRNAs and decrease their amplitude of circadian oscillation (Kim *et al.* 2005; Woo *et al.* 2008, 2010). Other proteins, identified as IRES *trans*-acting factors (ITAFs), enhance translation in a cap-independent manner. They trigger IRES-mediated translation of clock genes, as well as one tumor-suppressor gene, *p53* (Kim *et al.* 2007, 2010, 2013; Lee *et al.* 2011b). In addition to RNA-binding proteins, microRNAs have also been suggested as post-transcriptional regulators that control circadian rhythms (Cheng *et al.* 2007; Chen *et al.* 2013; Lee *et al.* 2013; Du *et al.* 2014).

In mammals, *Per* gene is widely expressed throughout every organ. All of the three paralogs, *Per1*, *Per2*, and *Per3*, display typical circadian mRNA oscillations and *Per1* and *Per2* are essential in the negative feedback loop via formation of heterodimer with *Cry1* and *Cry2*. However, they differentially function in various tissues. *Per1* and *Per2* are indispensable in the suprachiasmatic nucleus, a master clock located in the brain (Bae *et al.* 2001), while *Per*3 is important for the period and the phase of peripheral clocks located in pituitary, lung, adrenals, and so forth (Pendergast *et al.* 2012). The expression of *Per1* is entrained by external photic stimuli through the retinohypothalamic tract (RHT)-cyclic adenosine monophosphate (cAMP) pathway and by the BMAL1/CLOCK-mediated modulation through the auto-regulatory transcriptional feedback loop (Wilsbacher *et al.* 2002). In contrast, the expression of *Per3* is influenced only by the latter (Albrecht *et al.* 2001; Travnickova-Bendova *et al.* 2002). Furthermore, it is known that the polymorphism in *Per3* gene is related to the diurnal preference (Parsons *et al.* 2014), sleep homeostasis (Hasan *et al.* 2014), and delayed sleep phase syndrome (DSPS) (Ebisawa *et al.* 2001).

Despite the importance in gene expression and sleep physiology, little is known about how *Per3* mRNA is regulated. Additionally, it remains unclear how circadian oscillation of *Per3* mRNA is affected through the regulation of its stability compared to *Per1* and *Per2* (Woo *et al.* 2008). Recent studies demonstrated that 3′-UTR-mediated mRNA degradation is essential for mouse *Per3* (m*Per3*) mRNA oscillation (Kwak *et al.* 2006). Specifically, heterogeneous nuclear ribonucleoprotein (hnRNP) Q was identified as a modulator for 5′- and 3′-UTR-mediated phase-dependent translation, which is coupled to m*Per3* mRNA decay (Kim *et al.* 2011). Nonetheless, there is no evidence of *trans*-acting factors that bind directly to the *cis*-acting element in the 3′-UTR of m*Per3* mRNA and lead to mRNA decay.

The theoretical analysis using mathematical models has been widely used to analyze the complex phenomena in biological systems. Mathematical models provide theoretical insight and systemic understanding with less need for further experiments. Various mathematical models have been designed to simulate a range of biological systems from a single cell to a tissue. The latter models consist of highly interconnected neurons and are used to describe circadian oscillations in bacteria, flies, and mammals (Leloup *et al.* 1999; Forger and Peskin 2003; Leloup and Goldbeter 2004; Bernard *et al.* 2007). Although they could explain the robustness of 24-h-period against various external perturbations, few of them except a recent study, describing nonsense-mediated decay (NMD) by auto-regulated RNA-binding protein in the circadian rhythm of plants (Schmal *et al.* 2013), include post-transcriptional effects despite significant experimental evidence that post-transcriptional controls contribute to clock mRNA oscillations. Furthermore, most of the mathematical models describing circadian rhythms lack direct correspondence to biological experiments.

Here, we identify *trans*-acting factors that contribute to 3′-UTR-mediated stability regulation of m*Per3* mRNA. We show that the binding of a stabilizer or a destabilizer to m*Per3* 3′-UTR influences its stability and oscillation profile. Moreover, with the help of a mathematical model based on our experimental results, we demonstrate that the modulation of mRNA stability by 3′-UTR-binding proteins is critical for the amplitude of circadian m*Per3* mRNA oscillation.

Methods

Plasmids

The pcNAT reporter containing full-length m*Per3* 3′-UTR and pSK vectors containing serially deleted m*Per3* 3′-UTR for *in vitro* transcription were used as described previously (Kwak *et al.* 2006). Each of UTR-containing constructs was inserted into the *Eco*RI/*Xba*I restriction enzyme site and linearized by digestion with *Xba*I. For purification of Glutathione *S*-transferase (GST)-tagged recombinant proteins, the coding regions of mouse hnRNP K and polypyrimidine tract-binding protein (PTB) isoform 1 and 2 were amplified and digested with *Sal*I/*Not*I, and cloned into *Sal*I/*Not*I sites of pGEX-4T-3 vector (GE Healthcare Life Sciences, Uppsala, Sweden).

Cell culture and dexamethasone treatment

NIH-3T3, Neuro2A, and HEK293A cells were maintained in Dulbecco's modified Eagle's medium (HyClone, Logan, UT, USA) supplemented with 10% fetal bovine serum (HyClone) and 1% penicillin–streptomycin (Welgene, Daegu, Republic of Korea) in a humidified atmosphere containing 5% CO_2 at 37°C. The circadian phase of NIH-3T3 cells was synchronized by 100 nM dexamethasone (Dex.) treatment. After 2 h, the medium was replaced with complete medium.

Purification of recombinant proteins

GST-tagged recombinant proteins were obtained using the pGEX-4T-3 system. pGEX vectors containing all isoforms of mouse hnRNP K, PTB, and hnRNP D were transformed into *Escherichia coli* BL21 following protein induction by adding 0.5 mM of isopropyl-1-thio-β-D-galactopyranoside (IPTG) and incubated for 2 h at 37°C or 16 h at 18°C. The recombinant proteins were purified using glutathione-Sepharose-4B resin (GE Healthcare Life Sciences) and eluted from the beads with reduced glutathione according to the manufacturer's instructions.

In vitro transcription, UV cross-linking, immunoprecipitation, and RNA affinity purification

For UV cross-linking, [^{32}P]UTP (PerkinElmer, Waltham, MA, USA)-labeled RNA was transcribed from the *Xba*I-linearized pSK-m*Per3* 3′-UTR plasmid using T7 RNA polymerase (Promega, Madison, WI, USA). About 30 μg of cytoplasmic extracts prepared from NIH-3T3 cells or 1 μg of recombinant proteins were incubated with radiolabeled m*Per3* 3′-UTR RNAs in a 30 μL of binding mixture containing 0.5 mM dithiothreitol (DTT), 5 mM HEPES (pH 7.6), 75 mM KCl, 2 mM $MgCl_2$, 0.1 mM EDTA, 4% glycerol, 20 U recombinant RNasin ribonuclease inhibitor (Promega), and 4 μg of tRNA for 20 min at 30°C. After incubation, the mixtures were UV irradiated on ice for 15 min with a CL-1000 UV-crosslinker (UVP, Upland, CA, USA), and unbound RNAs were digested with 5 μL RNase cocktail [2.5 μL of RNase A (10 mg/mL; Roche Diagnostics, Indianapolis, IN, USA) and 2.5 μL of RNase T1 (100 U/mL; Roche Diagnostics)] for 50 min at 37°C. UV cross-linked proteins were analyzed by autoradiography after sodium dodecyl sulfate-polyacrylamide gel electrophoresis (SDS-PAGE). For immunoprecipitation, RNase-digested lysates were incubated with IgG or specific antibodies for 16 h at 4°C. After incubation, protein G agarose beads (Roche Diagnotics) were added and further incubated for 3 h at 4°C. Washed beads were analyzed by SDS-PAGE and autoradiography. For streptavidin-biotin RNA affinity purification, biotin-UTP-labeled RNA was transcribed from the *Xba*I-linearized pSK-m*Per3* 3′-UTR plasmid using T7 RNA polymerase. About 1 mg of pre-cleared cytoplasmic extracts from NIH-3T3 cells were incubated with biotinylated-m*Per3* 3′-UTR RNAs in a dialysis buffer containing 10 mM HEPES (pH 7.4), 90 mM KOAc, 1.5 mM MgOAc, 2.5 mM DTT, and tRNA for 30 min at 23°C. The binding mixtures were subjected to streptavidin resin adsorption for 16 h at 4°C. Resin-bound proteins were analyzed by SDS-PAGE.

RNA–immunoprecipitation

Immunoprecipitation was performed with a buffer containing 125 mM KCl, 20 mM HEPES (pH 7.4), 0.5 mM EDTA, 0.5 mM DTT, 0.5 mM phenylmethylsulfonyl fluoride (PMSF), 0.05% NP-40, and RNasin. About 1 μg of pre-immune serum or specific antibodies were incubated with RNase-free lysates for 2 h at 4°C. After incubation, 50 μL of protein G agarose bead was added and further incubated 16 h at 4°C. Washed beads were analyzed by SDS-PAGE followed by immunoblot or subjected to RNA isolation using TRI reagent (Molecular Research Center, Cincinnati, OH, USA) according to the manufacturer's instructions.

Transient transfection and RNA interference

For siRNA transfection into NIH-3T3 cells, a microporator (Digital-Bio, Seoul, Republic of Korea) was used according to the manufacturer's instructions with a condition of 1235 V, 20 ms, and 2 pulses. For pcNAT plasmid transfection, Neuro2A and HEK293A cells were seeded in 6-well plates at a density of 1×10^6 cells per well and incubated for 24 h before transfection. Transfection was performed using Metafectene (Biontex, München, Germany) according to the manufacturer's instructions. About 24 h after incubation, cells were harvested for further experiments. siRNAs for endogenous hnRNP K and hnRNP D knockdown were purchased from Dharmacon, Lafayette, CO, USA (siGENOME SMARTpool HNRPK M-048992091 and HNRPD M-042940-00). siRNA for endogenous PTB knockdown was synthesized as follow: siPTB 5′-ACA-CCUGUGCCUAGCAAUATT-3′ (Bioneer, Daejeon, Republic of Korea).

Subcellular fractionation and immunoblot analysis

Cytoplasmic lysates were prepared from NIH-3T3 cells using hypotonic-lysis buffer containing 10 mM HEPES (pH 7.9), 10 mM KCl, 1.5 mM $MgCl_2$, 1 mM DTT, 0.2 mM PMSF, and 2.5% NP-40 at 4°C. Nuclei were obtained by centrifugation, and washed twice in the hypotonic-lysis buffer to avoid contamination of cytoplasmic proteins. Nuclear lysates were prepared using extraction buffer containing 20 mM HEPES (pH 7.9), 450 mM NaCl, 1.5 mM $MgCl_2$, 1 mM DTT, 0.2 mM PMSF, and 0.2 mM EDTA (pH 8.0)

at 4°C. Both lysates were followed by repeated freeze-thaws for complete disruption. Immunoblot analysis was performed using polyclonal anti-PTB, polyclonal anti-PER3, anti-hnRNP D (Millipore Corporation, Bedford, MA, USA), anti-14-3-3ζ, anti-Lamin-B (Santa Cruz Biotechnology, Dallas, TX, USA), anti-hnRNP K (Abcam, Cambridge, UK) and monoclonal anti-FLAG (Sigma, St Louis, MO, USA), anti-glyceraldehyde-3-phosphate dehydrogenase (GAPDH) (Millipore Corporation) primary antibodies and horseradish peroxidase-conjugated rat-, rabbit-specific (Bethyl Laboratories, Montgomery, TX, USA), and mouse-specific (Thermo Scientific, Rockford, IL, USA) secondary antibodies. Proteins were analyzed using SUPEX enhanced chemiluminescence (ECL) solution kit (Neuronex, Daegu, Republic of Korea) and LAS-4000 chemiluminescence detection system (Fujifilm, Tokyo, Japan), according to the manufacturer's instructions.

Northern blot analysis

Total RNA was isolated by using TRI reagent according to the manufacturer's instructions. About 10 mg of total RNA was size-separated by 1% agarose gel electrophoresis containing 0.66 M formaldehyde, transferred to nylon membranes (Pall Corporation, Port Washington, NY, USA), and hybridized with a randomly primed probe labeled with [^{32}P]dCTP (PerkinElmer). For detection of reporter mRNA, rat serotonin *N*-acetyltransferase (NAT)-coding region was used as probe. Radioactivity was analyzed by autoradiography.

Quantitative real-time reverse-transcription (RT) PCR

Total RNA was isolated by using TRI reagent and reverse transcribed using oligo-dT and ImProm-II reverse-transcription system (Promega) according to the manufacturer's instructions. The amount of mRNA was analyzed by quantitative real-time PCR (Applied Biosystems, Foster City, CA, USA) with the FastStart Universal SYBR Green Master Mix (Roche Diagnostics). A comparative C_t method was used for quantification.

Pulse-chase with 5-bromouridine

Pulse-chase with 5-bromouridine (5-BrU) was performed as described previously (Paulsen *et al.* 2014) with minor modifications. Briefly, cells were incubated in conditioned medium including 2 mM of 5-BrU (Sigma-Aldrich, St Louis, MO, USA) for 30 min at 37°C. After incubation, rinse plate with phosphate-buffered saline (PBS) twice, then the medium was changed by conditioned medium including 20 mM uridine (Sigma). Cells were harvested and subjected to RNA isolation using TRI reagent. Heat-denatured total RNA was incubated in gentle rotation for 1 h at 23°C with 2 μg of anti-BrdU antibody (BD Pharmingen, BD Biosciences, San Jose, CA, USA) in diethylpyrocarnonate (DEPC)-treated PBS containing 0.1% bovine serum albumin (BSA) and 40 U RNasin. 5-BrU-labeled RNA captured by anti-BrdU antibody was immunoprecipitated by Protein G agarose, followed by phenol-chloroform extraction and EtOH down. Pellet was resuspended in DEPC-treated water and analyzed by quantitative real-time reverse-transcription PCR.

Mathematical modeling

To model a circadian clock with a fixed period against mRNA stability modulation, we considered two negative feedback loops based on the previous mathematical model with several modifications (Gonze and Goldbeter 2006). The model assumed that each of loops for transcriptional activator (stabilizing loop) and repressor (core loop) consists of three variables – mRNA (M), cytoplasmic protein (P_C), and nuclear protein (P_N) – and nuclear protein represses the synthesis of mRNA. Clock proteins (PC_P, PN_P, PC_{BC}, and PN_{BC}) shuttle between nuclear and cytoplasm, and clock gene mRNAs (M_P and M_{BC}) and cytoplasmic proteins (PC_P and PC_{BC}) are degradable. In addition, the nuclear protein in the stabilizing loop (PN_{BC}) induces the transcription of mRNA in the core loop (M_P). The equations in the model are as follows:

$$\frac{d[\mathrm{M}_{BC}]}{dt} = v_{sBC}\frac{\mathrm{KI}_{BC}{}^{n_{BC}}}{\mathrm{KI}_{BC}{}^{n_{BC}} + [\mathrm{PN}_{BC}]^{n_{BC}}} - v_{mBC}\frac{[\mathrm{M}_{BC}]}{\mathrm{K}_{mBC} + [\mathrm{M}_{BC}]} \quad (1)$$

$$\frac{d[\mathrm{PC}_{BC}]}{dt} = k_{sBC}[\mathrm{M}_{BC}] - v_{dBC}\frac{[\mathrm{PC}_{BC}]}{\mathrm{K}_{dBC} + [\mathrm{PC}_{BC}]} - k_{inBC}[\mathrm{PC}_{BC}] + k_{outBC}[\mathrm{PN}_{BC}] \quad (2)$$

$$\frac{d[\mathrm{PN}_{BC}]}{dt} = k_{inBC}[\mathrm{PC}_{BC}] - k_{outBC}[\mathrm{PN}_{BC}] \quad (3)$$

$$\frac{d[\mathrm{M}_P]}{dt} = v_{sP}\frac{[\mathrm{PN}_{BC}]}{\mathrm{K}_{aP} + \frac{[\mathrm{PN}_P]}{1+\mathrm{K}_{rP}[\mathrm{PN}_{BC}]}} - v_{mP}\frac{[\mathrm{M}_P]}{\mathrm{K}_{mP} + [\mathrm{M}_P]} \quad (4)$$

$$\frac{d[\mathrm{PC}_P]}{dt} = k_{sP}[\mathrm{M}_P] - v_{dP}\frac{[\mathrm{PC}_P]}{\mathrm{K}_{dP} + [\mathrm{PC}_P]} - k_{inP}[\mathrm{PC}_P] - k_{outP}[\mathrm{PN}_P] \quad (5)$$

$$\frac{d[\mathrm{PN}_P]}{dt} = k_{inP}[\mathrm{PC}_P] - k_{outP}[\mathrm{PN}_P] \quad (6)$$

The squared brackets indicate the concentration of associated components, and the variables in the equations represent the following species: M_{BC}, transcriptional activator mRNA; PC_{BC}, cytoplasmic transcriptional activator protein; PN_{BC}, nuclear transcriptional activator protein; M_P, transcriptional repressor mRNA; PC_P, cytoplasmic transcriptional repressor protein; PN_P, nuclear transcriptional repressor protein. The parameter values for the model are from ones used in previous studies (Gonze and Goldbeter 2006) with additional parameters reflecting the nature of two interlocked feedback loops as follows: $v_{sBC} = 2.15$, $KI_{BC} = 1$, $n_{BC} = 4$, $v_{mBC} = 0.505$, $K_{mBC} = 0.5$, $k_{sBC} = 0.5$, $v_{dBC} = 1.4$, $K_{dBC} = 0.13$, $k_{inBC} = 0.5$, $k_{outBC} = 0.6$, $v_{sP} = 0.1$, $K_{aP} = 10$, $K_{rP} = 10$, $v_{mP} = 0.2$, $K_{mP} = 0.2$, $k_{sP} = 1$, $v_{dP} = 1$, $K_{dP} = 0.15$, $k_{inP} = 0.5$, $k_{outP} = 0.6$. To test the effect of stable or unstable mRNA in the model, v_{mP} was halved or doubled. Simulation was performed using MATLAB (The Mathworks, Natick, MA, USA), and the ordinary differential equations were numerically analyzed using the 4th-order Runge-Kutta method.

Statistical analysis

Two-way ANOVA was performed to analyze the knockdown effect of different siRNAs throughout circadian times, followed by Bonferroni *post hoc* test using GraphPad Prism 6.03 for Windows (GraphPad Software Inc., La Jolla, CA, USA). The p values below 0.05 were considered significant. The results are expressed as mean ± SEM. CircWave (courtesy of Dr Roelof A. Hut) was used to analyze the rhythmicity of circadian m*Per3* mRNA expression (Statistics calculated by Circwave is summarized in Table S3).

Results

Circadian phase-dependent m*Per3* mRNA degradation

To examine the phase-dependent m*Per3* mRNA stability regulation by 3′-UTR-binding proteins, we disturbed the transcription of m*Per3* mRNA at different circadian phases. After Dex. treatment, m*Per3* mRNA exhibited a periodic oscillation (Fig. 1a); we observe a peak at 24 h after synchronization and a trough at 36 h after synchronization. When treated with actinomycin D (Act.D) at 28 h after synchronization (declining phase) or at 40 h after synchronization (rising phase), m*Per3* mRNA displayed different decay kinetics. The decay rate of m*Per3* mRNA normalized to mouse *Ribosomal protein L32* (m*Rpl32*) at the declining phase was much faster than the decay rate at rising phase (Fig. 1b). In contrast, the decay rate of mouse *TATA-box-binding protein* (m*Tbp*) mRNA was constant in both cases (Fig. 1c). Since the 3′-UTR is believed to be important for mRNA stability and m*Per3* mRNA has a known *cis*-acting element in 3′-UTR which is essential for its stability (Kwak *et al.* 2006), we assume that certain proteins bind to the *cis*-acting element in m*Per3* 3′-UTR and regulate the m*Per3* mRNA stability in a circadian phase-dependent manner.

Identification of m*Per3* 3′-UTR-binding proteins

To identify specific proteins that bind to m*Per3* 3′-UTR, a set of deletion constructs covering the *cis*-acting element identified in the previous study (Kwak *et al.* 2006) was generated (Fig. 2a). Cytoplasmic lysates were prepared from NIH-3T3 cells and subjected to *in vitro* binding assays. Protein bands of 57 and 43 kDa (p57 and p43) were almost disappeared when incubated with a construct that lacks the *cis*-acting element (Fig. 2b, lane 5); even though p57 was dramatically decreased when 1056 nucleotides were removed from 3′ of the full-length construct (Fig. 2b, lanes 1 and 2). This result indicates that the region of nucleotides 382–561 is indeed a

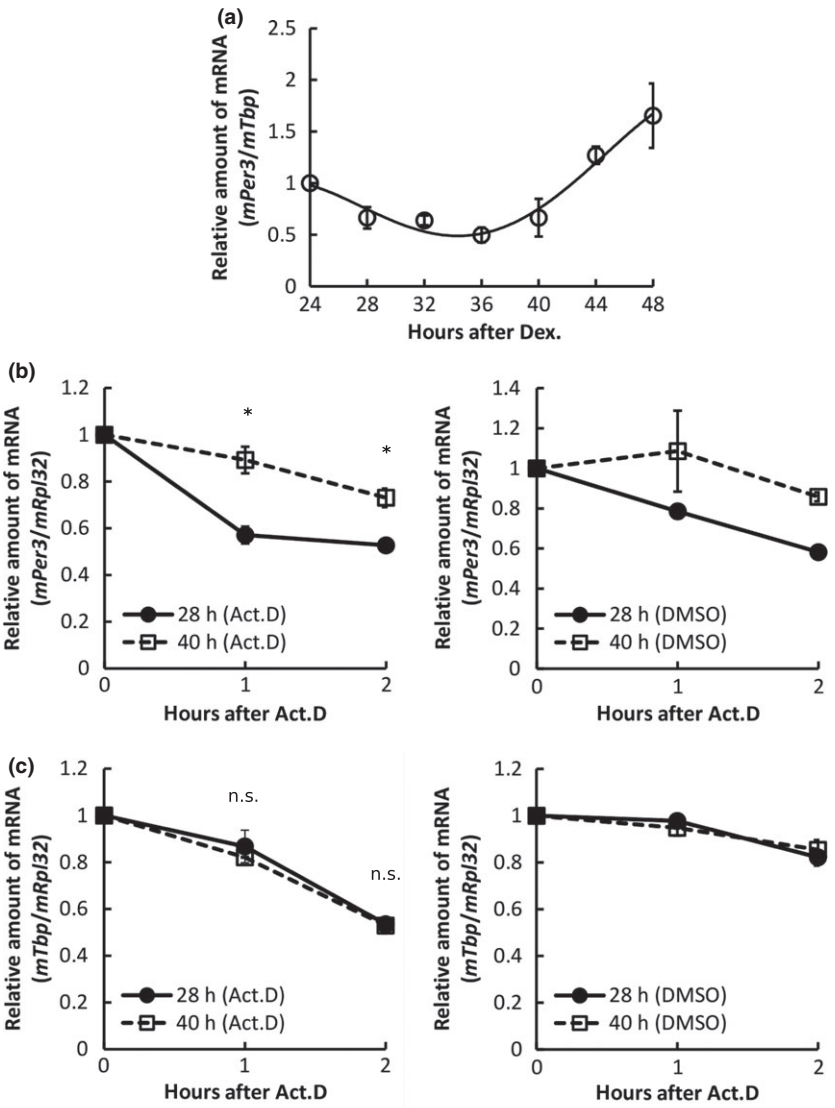

Fig. 1 m*Per3* mRNA is degraded in a circadian phase-dependent manner. (a) Part of the circadian expression of endogenous m*Per3* mRNA. NIH-3T3 cells were synchronized and harvested at indicated times. Total RNA was isolated and analyzed by quantitative real-time reverse-transcription (RT) PCR. The amount of m*Per3* mRNA was normalized to the level of m*Tbp* mRNA, and the initial amount of m*Per3* mRNA was arbitrarily set to 1. Error bars represent the SEM of three independent experiments. (b and c) Decay kinetics of endogenous m*Per3* (b) and m*Tbp* (c) mRNA. NIH-3T3 cells were synchronized by dexamethasone (Dex.) treatment. About 28 or 40 h after synchronization, actinomycin D (Act.D) was treated to the cells for the decay kinetics of m*Per3* mRNA in the declining (filled circles and solid line) or the rising (open squares and dashed line) phase, respectively. Vehicle (DMSO)-treated control for each of mRNAs are shown in right panels. The amount of m*Per3* (b) and m*Tbp* (c) mRNA was analyzed by quantitative real-time RT PCR and normalized to the level of m*Rpl32* mRNA. The initial amount of m*Per3* (b) and m*Tbp* (c) mRNA was arbitrarily set to 1. Error bars represent the SEM of three independent experiments (*$p < 0.05$; n.s. not significant).

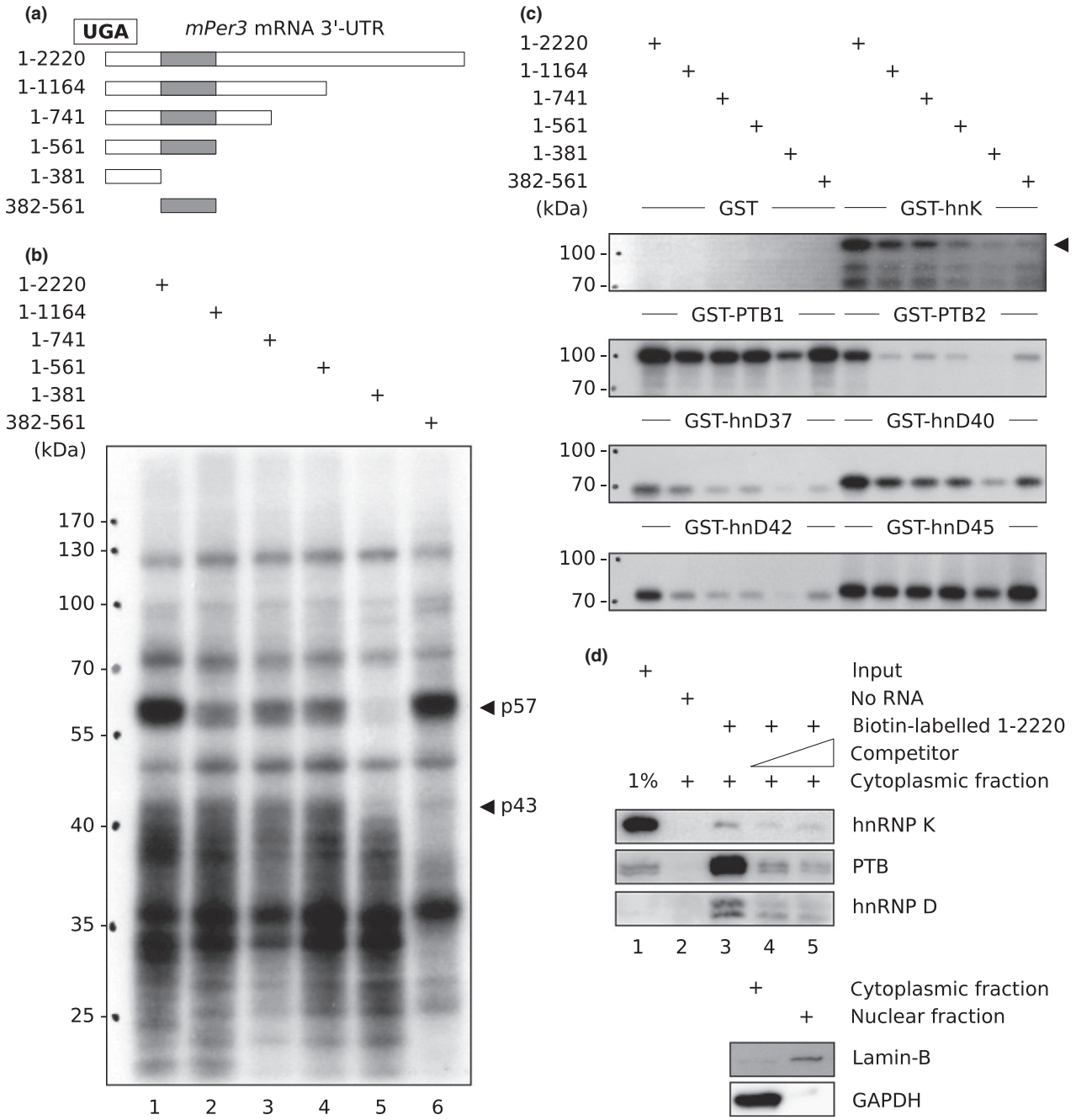

Fig. 2 Heterogeneous nuclear ribonucleoprotein (hnRNP) K, polypyrimidine tract-binding protein (PTB), and hnRNP D bind to m*Per3* 3′-UTR. (a) Schematic representation of pcNAT reporters containing either full-length m*Per3* 3′-UTR or its fragments. Stop codon of serotonin *N*-acetyltransferase (NAT)-coding region and nucleotide numbers of each constructs are shown. *Cis*-acting elements are indicated as gray squares. (b) UV cross-linking analysis between radiolabeled m*Per3* 3′-UTR serial deletion constructs and cytoplasmic lysates prepared from NIH-3T3 cells. ^{32}P-labeled RNA-protein complexes were UV cross-linked, digested by RNase and subjected to sodium dodecyl sulfate-polyacrylamide gel electrophoresis (SDS-PAGE). The arrowheads on the right indicate the 57 (p57) and 43 (p43) kDa proteins bound to the *cis*-acting element. Molecular mass markers are shown on the left in kilodaltons. (c) UV cross-linking analysis between radiolabeled m*Per3* 3′-UTR serial deletion constructs and glutathione *S*-transferase (GST)-tagged recombinant proteins. The arrowhead on the right represents GST-tagged mouse hnRNP K. Molecular mass markers are shown on the left in kilodaltons. (d) Streptavidin-biotin RNA affinity purification analysis between biotin-labeled m*Per3* 3′-UTR full-length construct and cytoplasmic lysates prepared from NIH-3T3 cells. Fivefold and 10-fold-unlabeled RNAs were co-incubated for competition of the interaction (lanes 4 and 5). Lamin-B and glyceraldehyde-3-phosphate dehydrogenase (GAPDH) were used as a nuclear and a cytoplasm marker, respectively.

putative-binding site of m*Per3* mRNA stability modulators. Using MALDI-TOF mass spectrometry with streptavidin-biotin RNA purified samples, p57 corresponded to two proteins, identified as hnRNP K and PTB, and p43 was identified as hnRNP D. The binding was confirmed by UV cross-linking and immunoprecipitation with specific antibodies (Figure S1a, lanes 7 to 10). Using autoradiography, we found that RNase-digested ^{32}P-labeled m*Per3* 3′-UTR full-length fragments co-immunoprecipitated with hnRNP K and PTB with an apparent molecular weight of 57 kDa. Likewise, ^{32}P-labeled fragments co-immunoprecipitated with hnRNP D at a molecular weight of 43 kDa. GST-tagged recombinant proteins were used to confirm *cis*-acting element-specific binding. In addition to hnRNP K, all isoforms of mouse PTB (PTB1; PTBP1 isoform 1 and PTB2; PTBP1 isoform 2, not a neuronal PTB – nPTB or PTBP2) and hnRNP D (hnD37, hnD40, hnD42, and hnD45) were purified by GST pull-down. The samples were then subjected to UV cross-linking with the set of radiolabeled m*Per3* 3′-UTR deletion constructs. The autoradiographs showed that hnRNP K, all isoforms of PTB, and hnRNP D bind to various regions on m*Per3* 3′-UTR. Moreover, all they bind directly to the *cis*-acting element in m*Per3* 3′-UTR, while purified GST protein did not bind to m*Per3* 3′-UTR (Fig. 2c, Figure S1b). Binding between m*Per3* 3′-UTR and hnRNPs was also verified by streptavidin-biotin RNA affinity purification analysis. Cytoplasmic hnRNP K, PTB, and hnRNP D were bound to biotin-labeled full-length m*Per3* 3′-UTR, and their specific binding to m*Per3* 3′-UTR was confirmed by competition analysis with unlabeled 3′-UTR, that gradually decreased as the amount of competitor was increased (Fig. 2d). These results suggest that hnRNP K, PTB, and hnRNP D directly bind to the *cis*-acting element in m*Per3* 3′-UTR.

Role of m*Per3* 3′-UTR-binding proteins in mRNA stability modulation

In the previous report, nucleotides 382–561 in m*Per3* 3′-UTR was identified as the *cis*-acting element for post-transcriptional mRNA decay (Kwak *et al.* 2006), and we identified hnRNP K, PTB, and hnRNP D as the *cis*-acting element-binding proteins. To examine their role in m*Per3* mRNA stability regulation, Neuro2A and HEK293A cells were transiently transfected with siRNAs for knockdown (Fig. 3a) or with expression vectors for over-expression (Fig. 3b) of each identified *trans*-acting factors, respectively. Furthermore, using NAT reporter plasmids without or with full-length m*Per3* 3′-UTR (NAT or NAT 3′-UTR), we investigated the stability of reporter mRNA-containing m*Per3* 3′-UTR. Northern blot analysis revealed that the knockdown of m*Per3* 3′-UTR-binding proteins differentially influenced the stability of m*Per3* 3′-UTR-containing reporter mRNA. Compared to non-targeting siRNA (siCon) treatment (Fig. 3a, lanes 1 and 2 in lower panel), the knockdown of hnRNP K (sihnK) accelerated reporter mRNA degradation (Fig. 3a, lanes 3 and 4 in lower panel). On the other hand, the knockdown of hnRNP D (sihnD) attenuated reporter mRNA degradation (Fig. 3a, lanes 7 and 8 in lower panel), while the knockdown of PTB (siPTB) exhibited little effect on reporter mRNA stability (Fig. 3a, lanes 5 and 6 in lower panel).

The knockdown effect of m*Per3* 3′-UTR-binding proteins on the stability of m*Per3* mRNA was validated by 5-BrU pulse-chase analysis. Neuro2A cells were transiently transfected with siRNAs for knockdown of each of *trans*-acting factors (Figure S2a). Using the reporter plasmids pulse labeled with 5-BrU, we obtained the consistent result with northern blot analysis that 6 h after chase, the knockdown of hnRNP K dramatically reduced the amount of reporter mRNA (Figure S2b, lanes 5 and 6) compared to the treatment of non-targeting control siRNA (Figure S2b, lanes 3 and 4), while the knockdown of hnRNP D did not make any decrease in the amount of reporter mRNA (Figure S2b, lanes 9 and 10).

The over-expression of m*Per3* 3′-UTR-binding proteins also displayed the differential reporter mRNA stability regulation. The amount of NAT reporter mRNA lacking m*Per3* 3′-UTR remained as a constant level after 6-h-actinomycin D treatment as reported previously (Kwak *et al.* 2006) (Fig. 3b, lanes 1 and 2 in lower panel). Compared to mock transfection (Fig. 3b, lanes 3 and 4 in lower panel), the over-expression of hnRNP K (FLAG-hnK) decelerated the degradation of reporter mRNA-containing m*Per3* 3′-UTR (Fig. 3b, lanes 5 and 6 in lower panel). On the other hand, the over-expression of hnRNP D (FLAG-hnD) accelerated reporter mRNA degradation (Fig. 3b, lanes 9 and 10 in lower panel), while the over-expression of PTB (FLAG-PTB) showed no effect on reporter mRNA stability (Fig. 3b, lanes 7 and 8 in lower panel). From these knockdown and over-expression analyses, we suggest that hnRNP K stabilizes and hnRNP D destabilizes m*Per3* 3′-UTR-containing reporter mRNA, while PTB has no effect on the stability.

Interaction between binding proteins and m*Per3* mRNA 3′-UTR

Most of the hnRNPs shuttle between cytoplasm and nucleus, and post-transcriptional mRNA degradation is believed to occur in cytoplasm (Dreyfuss *et al.* 2002; Bevilacqua *et al.* 2003). For this reason, we hypothesized that the cytoplasmic abundance of hnRNP K, PTB, and hnRNP D is important in each protein's ability to modulate temporal stability regulation of target mRNAs. Immunoblot analysis with specific antibodies showed the rhythmic expression of cytoplasmic m*Per3* 3′-UTR-binding proteins (Figure S3a). During a circadian period synchronized by Dex. treatment, the amount of cytoplasmic hnRNP K was began to increase after 24 h and began to decrease after 36 h after synchronization. The phase of cytoplasmic PTB was similar to that of hnRNP K albeit less dramatic (Figure S3a), but the phase of cytoplasmic hnRNP K and PTB were reciprocal compared to the

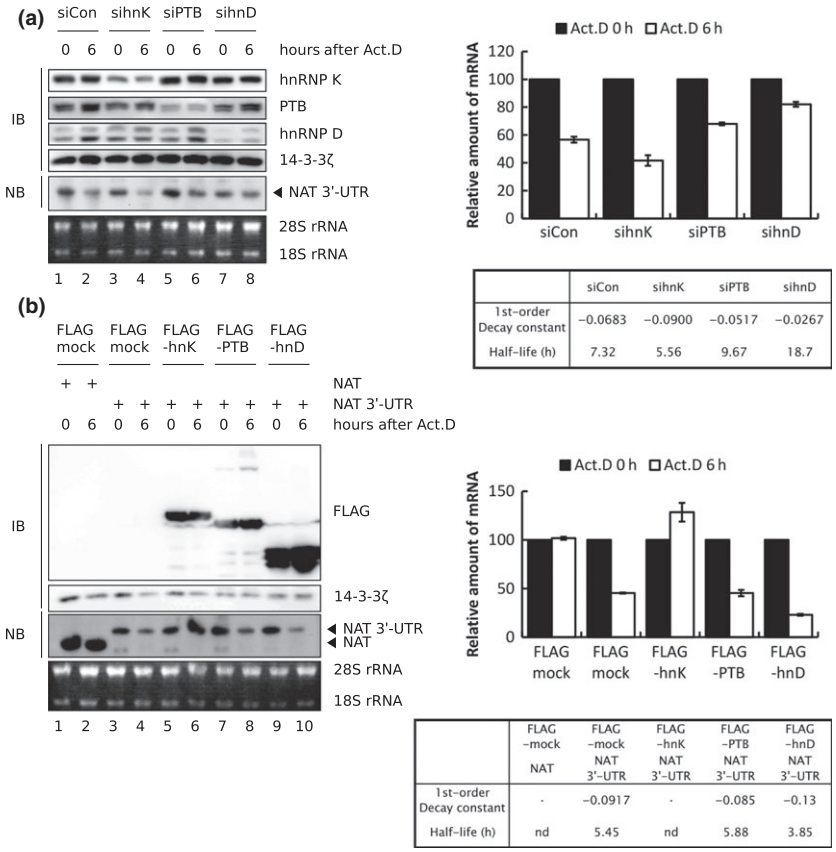

	siCon	sihnK	siPTB	sihnD
1st-order Decay constant	−0.0683	−0.0900	−0.0517	−0.0267
Half-life (h)	7.32	5.56	9.67	18.7

	FLAG −mock NAT	FLAG −mock NAT 3'-UTR	FLAG −hnK NAT 3'-UTR	FLAG −PTB NAT 3'-UTR	FLAG −hnD NAT 3'-UTR
1st-order Decay constant	·	−0.0917	·	−0.085	−0.13
Half-life (h)	nd	5.45	nd	5.88	3.85

Fig. 3 Heterogeneous nuclear ribonucleoprotein (hnRNP) K and hnRNP D modulate the stability of m*Per3* 3′-UTR-containing mRNA in an opposite manner. (a) Immunoblot and northern blot analysis for decay kinetics of m*Per3* 3′-UTR-containing mRNA according to the knockdown of 3′-UTR-binding proteins. Neuro2A cells were transiently transfected with siRNAs (siCon for non-targeting, sihnK for hnRNP K, siPTB for polypyrimidine tract-binding protein (PTB), and sihnD for hnRNP D). About 24 h after incubation, the cells were secondarily transfected with a reporter plasmid that m*Per3* 3′-UTR is inserted after serotonin *N*-acetyltransferase (NAT)-coding region (NAT 3′-UTR). Total RNA was isolated at indicated times after actinomycin D (Act.D) treatment, and analyzed using radiolabeled DNA probes against the NAT-coding sequence. The knockdown of corresponding proteins was confirmed with antibodies against hnRNP K, PTB, and hnRNP D. 14-3-3ζ was used as a loading control for immunoblot analysis. 28S and 18S rRNAs, stained with ethidium bromide, were used as loading controls for northern blot analysis. The band intensities normalized to the time zero of each knockdown conditions (odd lanes) were quantified and plotted (upper right, error bars represent SD of three technical replicates). First-order decay constants and mRNA half-lives were calculated and shown (lower right). (b) Immunoblot and northern blot analysis for decay kinetics of m*Per3* 3′-UTR-containing mRNA according to the over-expression of 3′-UTR-binding protein. HEK293A cells were transiently transfected with pFlag-CMV2 as a mock transfection (FLAG mock), and with pFlag-hnRNP K (FLAG-hnK), PTB (FLAG-PTB), and hnRNP D (FLAG-hnD). About 24 h after incubation, the cells were secondarily transfected with reporter plasmids that NAT-coding region only or that m*Per3* 3′-UTR is inserted after NAT-coding region (NAT or NAT 3′-UTR). Total RNA was isolated at indicated times after Act.D treatment, and detected using radiolabeled DNA probes against the NAT-coding sequence. The over-expression of corresponding proteins was confirmed with an antibody against FLAG. 14-3-3ζ was used as a loading control for immunoblot analysis. 28S and 18S rRNAs, stained with ethidium bromide, were used as loading controls for northern blot analysis. The band intensities normalized to the time zero of each over-expression conditions (odd lanes) were quantified and plotted (upper right, error bars represent SD of three technical replicates). First-order decay constants and mRNA half-lives were calculated and shown (lower right).

m*Per3* mRNA oscillation (Figs S3a and 1a). On the other hand, the phase of cytoplasmic hnRNP D, a trough at 28 h and a peak at 44 h after synchronization, was slightly delayed compared to the phase of hnRNP K and PTB.

This result led us to hypothesize that hnRNP K and PTB are acting in the declining phase (from the peak to the trough) of m*Per3* mRNA, and hnRNP D is acting in the rising phase (from the trough to the peak) of m*Per3* mRNA. To elucidate the rhythmic interaction between m*Per3* mRNA and 3′-UTR-binding proteins, *in vitro* binding assay with synchronized cytoplasmic lysates harvested at different points along the circadian phases was performed. Radiolabeled m*Per3*

3′-UTR full-length and *cis*-acting element was co-incubated with the cytoplasmic lysates of 28 h (a descent point of m*Per3* mRNA oscillation) and 40 h (an ascent point) after synchronization followed by UV cross-linking. The binding pattern between m*Per3* mRNA and 3′-UTR-binding proteins was not significantly different for both constructs (Figure S3b). The same result was observed when the cytoplasmic lysates were co-incubated with biotin-labeled m*Per3* 3′-UTR full-length or *cis*-acting element followed by streptavidin-biotin RNA affinity purification (Figure S3c). Since *in vitro* transcribed constructs were used, we performed an RNA-immunoprecipitation analysis, which has the advantage of observing the interaction between endogenous mRNA and protein. Cytoplasmic lysates prepared from Dex.-treated NIH-3T3 cells, and endogenous hnRNP K, PTB, and hnRNP D were immunoprecipitated with specific antibodies. Immunoprecipitated samples were subjected to RNA isolation and quantitative real-time reverse-transcription (RT) PCR for m*Per3*. Interestingly, the amount of hnRNP K-bound m*Per3* mRNA was slightly increased in the lysates prepared 24 h after synchronization that m*Per3* mRNA is maximally abundant. The amount of hnRNP D-bound m*Per3* mRNA was increased in the lysates collected 36 h after synchronization, the trough in m*Per3* mRNA expression (Figure S3d). Although PTB was likely to have a strong binding affinity to *mPer3* mRNA, the effect on mRNA stability regulation was negligible (Fig. 3a and b). From these results, we could not determine whether hnRNP K, PTB, and hnRNP D bind to m*Per3* mRNA3′-UTR in a circadian phase-dependent manner; therefore, the underlying mechanism how hnRNP K, PTB, and hnRNP D rhythmically regulate the stability of m*Per3* mRNA should be studied further.

Role of RNA-binding proteins in circadian m*Per3* mRNA expression

To verify the effect of stability regulation on the circadian mRNA oscillation, we analyzed endogenous m*Per3* mRNA oscillation according to the individual knockdown of hnRNP K, PTB, and hnRNP D. NIH-3T3 cells were transiently transfected with siRNAs for hnRNP K (sihnK), PTB (siPTB), or hnRNP D (sihnD), at 24 h before synchronization, then incubated for 48 additional hours (Fig. 4a). Compared to the transfection with non-targeting siRNA (siCon), the knockdown of hnRNP K significantly lowered the peak amplitude of m*Per3* mRNA oscillation ($p = 0.0225$), while the period and the phase of circadian oscillation remained unchanged

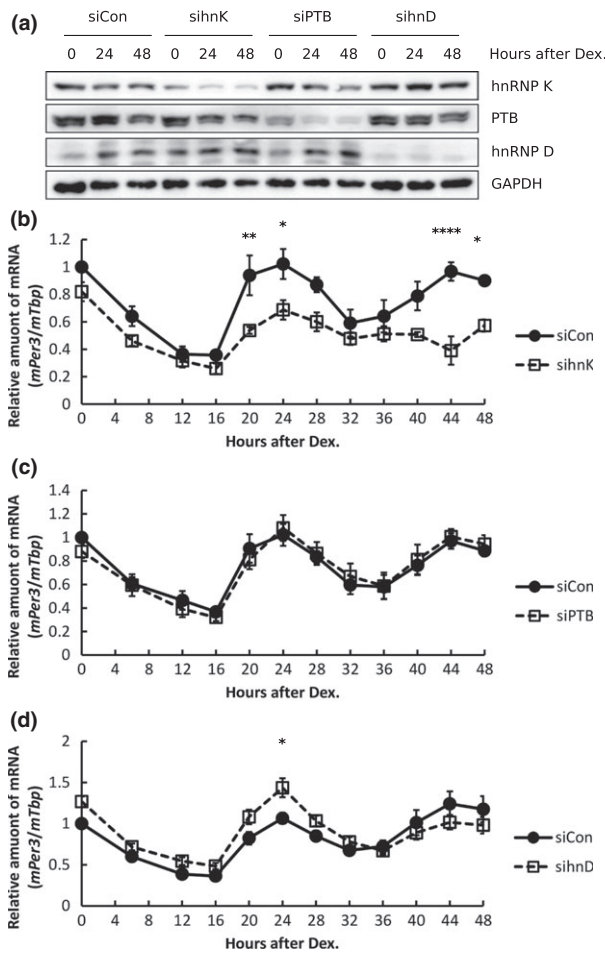

Fig. 4 Knockdown of heterogeneous nuclear ribonucleoprotein (hnRNP) K and hnRNP D affects the amplitude of circadian m*Per3* mRNA oscillation. (a) Immunoblot analysis for knockdown of *trans*-acting factors. NIH-3T3 cells were transiently transfected with siRNAs for non-targeting (siCon), hnRNP K (sihnK), polypyrimidine tract-binding protein (PTB) (siPTB), and hnRNP D (sihnD) at 24 h before synchronization. Cells were synchronized by dexamethasone (Dex.) treatment and harvested at indicated times. Proteins were analyzed by antibodies against hnRNP K, PTB, and hnRNP D. Glyceraldehyde-3-phosphate dehydrogenase (GAPDH) was used as a loading control. (b) Temporal expression of m*Per3* mRNA affected by the knockdown of hnRNP K. NIH-3T3 cells were transiently transfected with siRNAs for non-targeting (siCon; filled diamonds and solid line) or hnRNP K (sihnK; open squares and dashed line) 24 h before synchronization. Cells were synchronized by Dex. treatment and harvested at indicated times. Total RNA was isolated and analyzed by quantitative real-time reverse-transcription (RT) PCR. The amount of m*Per3* mRNA was normalized to the level of m*Tbp*, and the initial amount of m*Per3* mRNA with siCon was arbitrarily set to 1. Error bars represent the SEM of four independent experiments (*$p < 0.05$; **$p < 0.01$; ****$p < 0.001$). (c) Temporal expression of m*Per3* mRNA affected by knockdown of PTB. NIH-3T3 cells were transiently transfected with siRNAs for non-targeting (siCon; filled diamonds and solid line) or PTB (siPTB; open triangles and dashed line) at 24 h before synchronization. Experimental procedures were same as described in panel (b). Error bars represent the SEM of five independent experiments. (d) Temporal expression of m*Per3* mRNA affected by knockdown of hnRNP D. NIH-3T3 cells were transiently transfected with siRNAs for non-targeting (siCon; filled diamonds and solid line) or hnRNP D (sihnD; open circles and dashed line) at 24 h before synchronization. Experimental procedures were same as described in panel (b). Error bars represent the SEM of ten independent experiments (*$p < 0.05$).

(Fig. 4b and Table S3). A dose-dependent sihnK treatment showed a dramatic decrease in m*Per3* mRNA oscillation (Figure S4a). This result indicates that hnRNP K is required not only for m*Per3* mRNA stabilization but also for amplitude formation. In contrast, the knockdown of PTB did not make any change in the period, phase, and amplitude of circadian m*Per3* mRNA oscillation (Fig. 4c and Table S3, $p = 0.9877$). Likewise, a dose-dependent siPTB treatment displayed no significant alteration in circadian m*Per3* mRNA oscillation despite a little fluctuation (Figure S4b). The effect of hnRNP D knockdown was restricted to the first period (Fig. 4d and Table S3, $p = 0.0033$). The amplitude of m*Per3* mRNA oscillation was significantly increased only at the first peak. A dose-dependent sihnD treatment also showed that the amplitude of m*Per3* mRNA oscillation was gradually increased only at the first peak, consistent with the initial experiment (Figure S4c). This result indicates that hnRNP D participates in the destabilization of m*Per3* mRNA, as well as the reduction in its circadian amplitude. The knockdown of hnRNP K and hnRNP D showed a partly opposite effect on circadian m*Per3* mRNA oscillation that the knockdown of hnRNP K decreased the amplitude of m*Per3* mRNA oscillation and the knockdown of hnRNP D increased it at the first peak. We examined whether the double knockdown recovered the amplitude of m*Per3* mRNA oscillation. NIH-3T3 cells were transiently transfected with siRNAs for hnRNP K, hnRNP D, and mix of two at 24 h before synchronization, and then incubated cells for 48 additional hours (Figure S5a). The oscillation of m*Per3* mRNA treated with siRNAs for non-targeting (siCon), hnRNP K (sihnK), and hnRNP D (sihnD) was consistent with the initial experiments (Fig. 4). Interestingly, the m*Per3* mRNA treated with siRNAs for both hnRNP K and hnRNP D (sihnKD) oscillated between m*Per3* mRNA of sihnK and that of sihnD except a single time point (Figure S5b). m*Per3* mRNA of sihnKD failed to recover to that of siCon, because the knockdown effect of hnRNP K on the amplitude of m*Per*3 mRNA oscillation was greater than that of hnRNP D (Fig. 4b and d).

Altogether, our results demonstrate that hnRNP K and hnRNP D control not only the stability of m*Per3* mRNA but also the amplitude of its circadian oscillation in an opposite manner, while PTB has no significant function.

Theoretical analysis between m*Per3* mRNA stability and its circadian oscillation

To confirm theoretically the effect of post-transcriptional mRNA stability regulation on its circadian oscillation, we developed a mathematical model consisting of two interlocked negative feedback loops as described in Methods. Each of the loops were called a stabilizing loop (for transcriptional activators: *Bmal1* and *Clock*) and a core loop (for transcriptional repressors: *Per3*) as described previously (Emery and Reppert 2004). They contained parameters for three variables that mRNA, cytoplasmic protein, and nuclear protein for each loop (Fig. 5a). The simulation result from the model with a suitable choice of parameters showed the circadian oscillations with a period of about 24 h for all components in each of loops (Fig. 5b, solid line). In addition, the model showed the circadian expression of cytoplasmic and nuclear mPER3 proteins and their phase relationship, as observed experimentally (data not shown). To investigate the alteration in circadian m*Per3* oscillation as the function of its stability, we increased or decreased the maximum rate of m*Per3* mRNA degradation (v_{mP}). As expected, the amplitude of m*Per3* mRNA oscillation was increased when stable (v_{mP} was decreased, Fig. 5b; dotted line), which corresponds to the knockdown of hnRNP D (Figs 3a and 4d). Likewise, the amplitude of m*Per3* mRNA oscillation was decreased when unstable (v_{mP} was increased, Fig. 5b; dashed line), which corresponds to the knockdown of hnRNP K (Figs 3a and 4b). Interestingly, the period of m*Per3* mRNA oscillation was constant even if the stability of m*Per3* mRNA was perturbed (Fig. 5d), while the amplitude showed a reciprocal relationship with the degradation rate of mRNA (Fig. 5c and Figure S6). This result cannot be obtained from a single negative feedback loop model, which shows a dependency between mRNA stability and the period of oscillation (Figure S7). Based on the results from the model, we can theoretically confirm the effect of post-transcriptional mRNA degradation on its oscillation profile, consistent with the results of experiments. Furthermore, we find that an additional negative feedback loop is required for the robustness of circadian period against the post-transcriptional modulation of mRNA stability.

Discussion

The circadian expression of clock genes originates from the interlocking negative feedback loops. A number of studies have focused on the transcriptional and the post-translational regulation of clock genes to describe their rhythmic expression. In other words, the rhythmic synthesis of clock gene mRNA through the rhythmic turnover of repressor proteins or the rhythmic dimerization of transcriptional activator proteins is considered as the core process in circadian rhythms. However, recent studies suggest that post-transcriptional regulation including mRNA decay and IRES-mediated translation also contributes to the clock gene expression. We suggest here that the circadian phase-dependent clock gene mRNA degradation modulated by RNA-binding proteins is important for the circadian expression of clock genes.

hnRNPs, one family of RNA-binding proteins, are well known for their function on RNAs during the process of mature mRNAs from pre-RNAs. In general, hnRNPs immediately bind to newly synthesized RNAs in the nucleus, and they participate in the preventing of RNA degradation, splicing of immature RNAs, and transporting of RNAs to cytoplasm (Dreyfuss *et al.* 2002). Moreover, several hnRNPs have been identified to have a post-transcriptional role in the stability

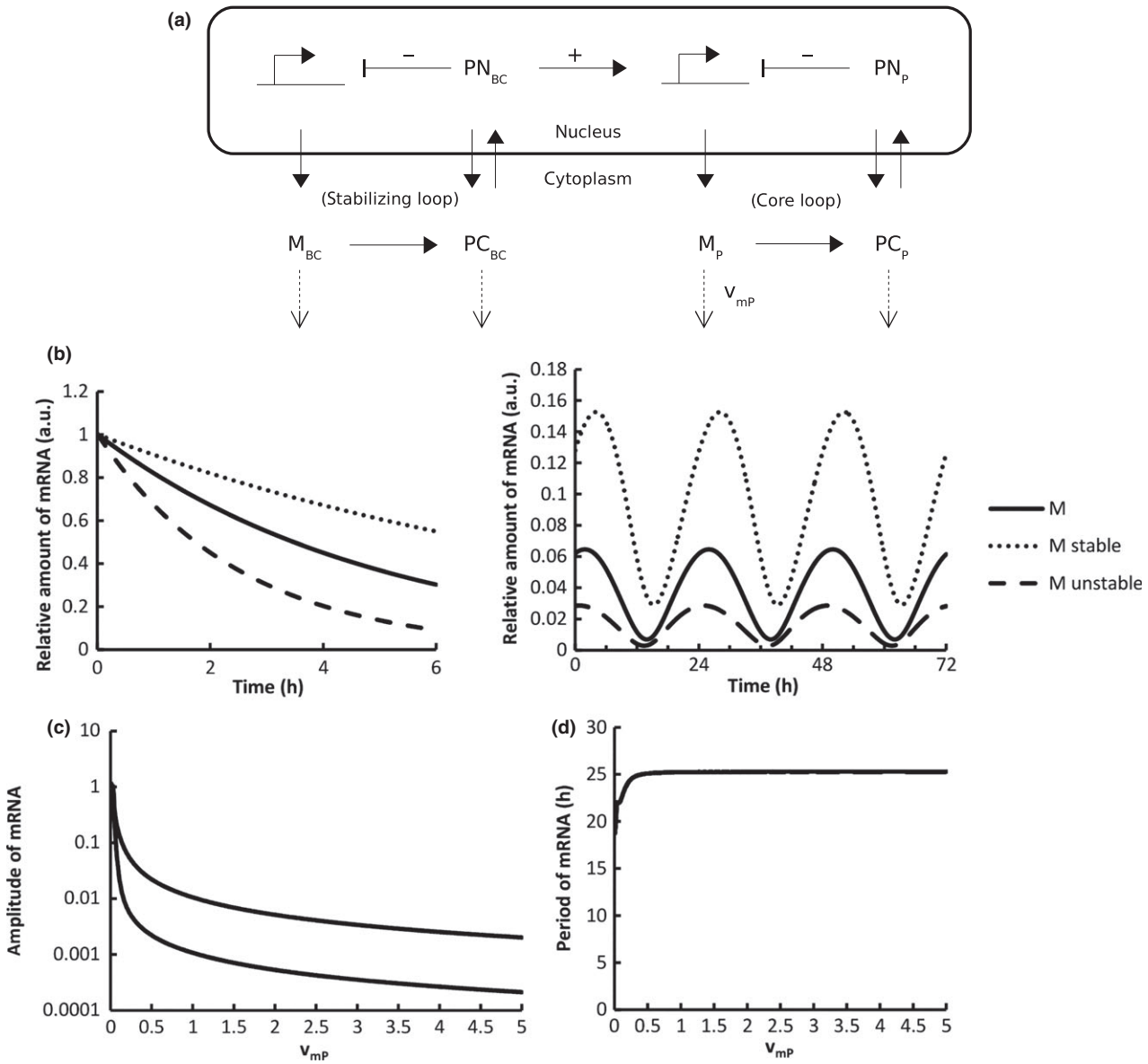

Fig. 5 Mathematical model for circadian m*Per3* expression shows the relation between mRNA stability and circadian oscillation. (a) Scheme of the model that consists of two negative feedback loops. The model is based on the effect of nuclear clock proteins (PN_{BC} and PN_P) as a transcriptional repressor of themselves (M_P and M_{BC}) and the effect of nuclear clock protein in the stabilizing loop (PN_{BC}) as a transcriptional activator of clock mRNA in the core loop (M_P). Clock mRNAs (M_P and M_{BC}) and cytoplasmic clock proteins (PC_P and PC_{BC}) are spontaneously degraded with their own decay rate. (b) mRNA decay kinetics and corresponding oscillation from the model. (Left) The initial amount of M_P was set to 1, and M_Ps with various maximum degradation rates were decreasing for 6 h. The dotted line indicates stable M_P (small v_{mP}) and the dashed line indicates unstable M_P (large v_{mP}). (Right) The amount of M_Ps with corresponding maximum degradation rates described in panel (a) was oscillating for 72 h. (c) Bifurcation diagram as the function of the maximum mRNA degradation rate v_{mP}. The curve shows the maximum and minimum amount of mRNA in a steady state. A stable limit cycle is appeared in the wide range of the v_{mP}, and the basal level of mRNA is decreased as the value of v_{mP} is increased. The *x*-axis indicates the degradation rate of mRNA (v_{mP}), and the *y*-axis indicates the amplitude of mRNA oscillation in a logarithmic scale. (d) Bifurcation diagram of period as the function of the maximum mRNA degradation rate v_{mP}. The curve shows the period of mRNA oscillation with the corresponding parameter value in a steady state. The *x*-axis indicates the degradation rate of mRNA (v_{mP}), and the *y*-axis indicates the period of mRNA oscillation.

control of clock gene mRNAs. hnRNP R, hnRNP Q, and hnRNP L accelerate *Nat* mRNA degradation (Kim *et al.* 2005); PTB and hnRNP D destabilize *Per2* and *Cry1*, respectively (Woo *et al.* 2008, 2010). In this study, we identified three proteins that bind to the *cis*-acting element located in the 3′-UTR of m*Per3* mRNA. Among them, hnRNP

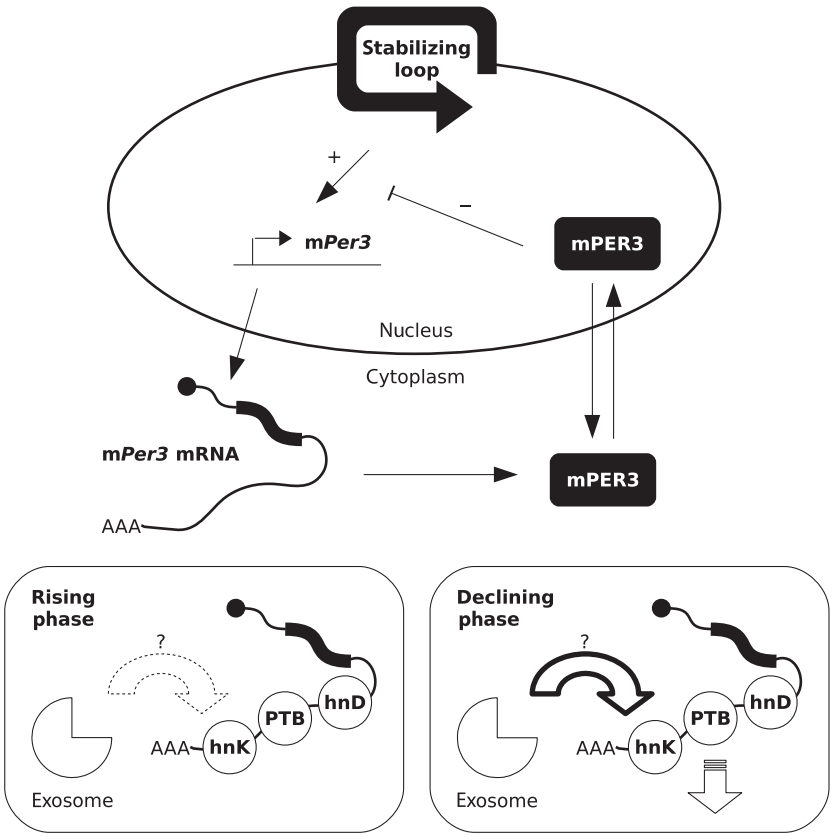

Fig. 6 Proposed model for the rhythmic modulation of m*Per3* mRNA stability and its circadian oscillation by heterogeneous nuclear ribonucleoprotein (hnRNP) K and hnRNP D. Proposed model for rhythmic degradation of m*Per3* mRNA modulated by hnRNP K, polypyrimidine tract-binding protein (PTB), and hnRNP D. The transcription of m*Per3* mRNA is induced by the stabilizing loop of transcription activators (e.g., Bmal1 and Clock). mPER3 protein shuttles between cytoplasm and nucleus, and the only nuclear mPER3 protein represses its transcription. hnRNP K, PTB, and hnRNP D are m*Per3* 3′-UTR-binding proteins and they regulate the stability of m*Per3* mRNA. Their binding to m*Per3* mRNA is constant; however, they recruit the RNA decay machinery (e.g., exosome) rhythmically through an unknown mechanism. (hnK, hnRNP K; hnD, hnRNP D; AAA, poly(A) tail).

K and hnRNP D are characterized as a stabilizer and a destabilizer for m*Per3* mRNA, respectively (Fig. 6). However, the underlying mechanism how hnRNPs regulate the stability of target mRNAs remains unclear. A possible destabilizing mechanism by hnRNP D was suggested in the recent study about the RNA-dependent interaction of guanosine triphosphate-binding protein1 (GTPBP1) (Woo *et al.* 2011). Since GTPBP1 directly binds to the components of exosome complex, which is 3′ to 5′ exoribonuclease, the binding of hnRNP D to m*Per3* mRNA 3′-UTR may result in the exosome-mediated mRNA degradation. In contrast, the stabilizing mechanism by hnRNP K is not fully understood despite some experimental observations that hnRNP K stabilizes ribosomal RNA in human pancreatic ductal epithelial cells (Wen *et al.* 2012) and extracellular signal-regulated kinases (ERK)-mediated cytoplasmic accumulation of hnRNP K increases the stability of thymidine phosphorylase mRNA (Chen *et al.* 2009). We suggest three possible stabilizing mechanisms of hnRNP K. First, hnRNP K shares a binding site with hnRNP D, therefore the binding of hnRNP K on target mRNA disturbs the binding of hnRNP D. Alternatively, the binding of hnRNP K on target mRNA may interfere with the recruitment of GTPBP1-associated exosome components by hnRNP D. The third possibility is that hnRNP K has an exosome-independent stabilizing mechanism.

Stability modulation by hnRNP K and hnRNP D affects the oscillation profile of m*Per3* mRNA. In this study, we identified that hnRNP K knockdown decreases the amplitude of m*Per3* mRNA oscillation through two full circadian periods (Fig. 4b). Alternatively, hnRNP D knockdown increases the amplitude of m*Per3* mRNA oscillation at the first peak (24 h after Dex. treatment), but the amplitude of m*Per3* mRNA nears normal levels during the second peak (48 h after Dex. treatment) as shown in Fig. 4d. This observation seems to be the result of the differential effect of 3′-UTR-binding proteins on the paralogs of clock gene mRNAs. Previously, a study suggested that the negative regulators of circadian clock, such as *Per*, *Cry*, and *Rev-erb*, have their own paralogs that exhibit structural or functional homology (*Per1*, *Per2*, and *Per3*; *Cry1* and *Cry2*; *Rev-erb* α and *Rev-erb* β). Moreover, it is believed that the disruption of clock gene expression is compensated and recovered by its paralogs; hence the robustness of circadian oscillations can be achieved (Baggs *et al.* 2009). In our study, the knockdown of hnRNP K lowers the overall amplitude of m*Per3* mRNA oscillation for 48 h. It is likely that the effect of hnRNP K knock-down widely influences the overall clock gene paralogs; therefore the circadian amplitude of m*Per3* mRNA oscillation becomes entirely dampened. In contrast, the knockdown of hnRNP D decreases the amplitude of the first peak but slightly increases that of the second peak of m*Per3* mRNA oscillation. It is likely that the effect of knock-down at the first peak became diminished and recovered during the second circadian period. In this case, the perturbation of

m*Per3* mRNA stability seems to be compensated by m*Per1* or m*Per2*. From these results, we conclude that the effect of post-transcriptional mRNA stability regulation is buffered by the feedback loops consisting of clock genes and their paralogs.

Several studies have reported the role of mRNA 3′-UTR-binding proteins and their cytoplasmic accumulation that influences mRNA stability and its oscillation profile in post-transcriptional way. For instance, the amount of cytoplasmic PTB strongly affects the amplitude and marginally affects the phase of m*Per2* mRNA (Woo *et al.* 2008). Furthermore, the amount of cytoplasmic hnRNP D controls the amplitude and phase of m*Cry1* mRNA to some extent (Woo *et al.* 2010). In this study, hnRNP K and hnRNP D influenced the stability and oscillation amplitude of m*Per3* mRNA in an opposite manner, while no alteration of period and phase was observed. Our results from the mathematical model suggest the underlying mechanism that an additional negative feedback loop is required for the robustness of a circadian period. BMAL1 and CLOCK form a heterodimer and function as a transcriptional activator for various clock genes. Notably, the synthesis of *Bmal1* mRNA by a transcriptional activator *retinoid-related orphan receptor* (*Ror*) and a transcriptional repressor *Rev-erb* is well understood (Guillaumond *et al.* 2005), while that of *Clock* remains unclear. We hypothesize that unless perturbed itself, the negative feedback loop of *Bmal1* generates and sustains the 24-h-period of clock gene mRNA oscillation. In our study, it is likely that the negative feedback loop of *Bmal1* is not altered by the m*Per3* mRNA stability modulation by the knockdown of hnRNP K and hnRNP D. Taken together, we conclude that a single negative feedback loop is insufficient for the robustness of circadian rhythms against post-transcriptional perturbation.

Acknowledgments and conflict of interest disclosure

We thank Dr Sangjune Kim, Hyo-Jin Kim, and Jung-Hyun Choi for critical discussion and reading of the manuscript. This work was supported by grants from the National Research Foundation of Korea (NRF) [2014054324]; Next-Generation BioGreen 21 Program [PJ00950302], Rural Development Administration; Brain Korea 21 Plus Program [10Z20130012243] of the Ministry of Education, Republic of Korea.

All experiments were conducted in compliance with the ARRIVE guidelines. The authors have no conflict of interest to declare.

Supporting information

Additional supporting information may be found in the online version of this article at the publisher's web-site:

Figure S1. hnRNP K, PTB, and hnRNP D bind to nucleotide 382-561 in m*Per3* mRNA 3'-UTR.

Figure S2. hnRNP K and hnRNP D modulate the stability of m*Per3* 3'-UTR-containing reporter mRNA.

Figure S3. m*Per3* mRNA interacts with cytoplasmic hnRNPs.

Figure S4. Dose-dependent treatment of siRNAs for hnRNP K and hnRNP D affect the amplitude of circadian m*Per3* mRNA oscillation.

Figure S5. Knockdown of hnRNP K and hnRNP D oppositely affects the amplitude of circadian m*Per3* mRNA oscillation.

Figure S6. Mathematical model for circadian m*Per3* expression shows the relation between mRNA stability and circadian oscillation.

Figure S7. Single negative feedback loop model for circaidan m*Per3* expression.

Table S1. Primer sequences for GST-tagged recombinant protein cloning.

Table S2. Oligo sequences for quantitative real-time RT PCR.

Table S3. Statistical parameters calculated by Circwave.

References

Akashi M., Tsuchiya Y., Yoshino T. and Nishida E. (2002) Control of intracellular dynamics of mammalian period proteins by casein kinase I epsilon (CKIepsilon) and CKIdelta in cultured cells. *Mol. Cell. Biol.* **22**, 1693–1703.

Albrecht R. (2012) Timing to perfection: the biology of central and peripheral circadian clocks. *Neuron* **74**, 246–260.

Albrecht U., Zheng B., Larkin D., Sun Z. S. and Lee C. C. (2001) MPer1 and mper2 are essential for normal resetting of the circadian clock. *J. Biol. Rhythms* **16**, 100–104.

Asher G., Gatfield D., Stratmann M., Reinke H., Dibner C., Kreppel F., Mostoslavsky R., Alt F. W. and Schibler U. (2008) SIRT1 regulates circadian clock gene expression through PER2 deacetylation. *Cell* **134**, 317–328.

Bae K., Jin X., Maywood E. S., Hastings M. H., Reppert S. M. and Weaver D. R. (2001) Differential functions of mPer1, mPer2, and mPer3 in the SCN circadian clock. *Neuron* **30**, 525–536.

Baggs J. E., Price T. S., DiTacchio L., Panda S., Fitzgerald G. A. and Hogenesch J. B. (2009) Network features of the mammalian circadian clock. *PLoS Biol.* **7**, e52.

Bass J. and Takahashi J. S. (2010) Circadian integration of metabolism and energetics. *Science* **330**, 1349–1354.

Bernard S., Gonze D., Cajavec B., Herzel H. and Kramer A. (2007) Synchronization-induced rhythmicity of circadian oscillations in the suprachiasmatic nucleus. *PLoS Comput. Biol.* **3**, e68.

Bevilacqua A., Ceriani M. C., Capaccioli S. and Nicolin A. (2003) Post-transcriptional regulation of gene expression by degradation of messenger RNAs. *J. Cell. Physiol.* **195**, 356–372.

Busina L., Bassermann F., Maiolica A., Lee C., Nolan P. M., Godinho S. I., Draetta G. F. and Pagano M. (2007) SCFFbxl3 controls the oscillation of the circadian clock y directing the degradation of cryptochrome proteins. *Science* **316**, 900–904.

Chen L. C., Liu H. P., Li H. P., Hsueh C., Yu J. S., Liang C. L. and Chang Y. S. (2009) Thymidine phosphorylase mRNA stability and protein levels are increased through ERK-mediated cytoplasmic accumulation of hnRNP K in nasopharyngeal carcinoma cells. *Oncogene* **28**, 1904–1915.

Chen R., D'Alessandro M. and Lee C. (2013) miRNAs are required for generating a time delay critical for the circadian oscillator. *Curr. Biol.* **23**, 1959–1968.

Cheng H. Y., Papp J. W., Varlamova O. *et al.* (2007) microRNA modulation of circadian-clock period and entrainment. *Neuron* **54**, 813–829.

Dardente H., Mendoza J., Fustin J. M., Challet E. and Hazlerigg D. G. (2008) Implication of the F-Box Protein FBXL21 in circadian pacemaker function in mammals. *PLoS ONE* **3**, e3530.

Dreyfuss G., Kim V. N. and Kataoka N. (2002) Messenger-RNA-binding proteins and the messages they carry. *Nat. Rev. Mol. Cell Biol.* **3**, 195–205.

Du N. H., Arpat A. B., De Matos M. and Gatfield D. (2014) MicroRNAs shape circadian hepatic gene expression on a transcriptome-wide scale. *Elife* **3**, e02510.

Ebisawa T., Uchiyama M., Kajimura N., Mishima K., Kamei Y., Katoh M., Watanabe T., Sekimoto M., Shibui K. and Kim K. (2001) Association of structural polymorphisms in the human period3 gene with delayed sleep phase syndrome. *EMBO Rep.* **2**, 342–346.

Emery P. and Reppert S. M. (2004) A rhythmic Ror. *Neuron* **43**, 443–446.

Forger D. B. and Peskin C. S. (2003) A detailed predictive model of the mammalian circadian clock. *Proc. Natl Acad. Sci. USA* **100**, 14806–14811.

Gekakis N., Stakins D., Nguyen H. B., Davis F. C., Wilsbacher L. D., King D. P., Takahashi J. S. and Weitz C. J. (1998) Role of the CLOCK protein in the mammalian circadian mechanism. *Science* **280**, 1564–1569.

Gonze D. and Goldbeter A. (2006) Circadian rhythms and molecular noise. *Chaos* **16**, 026110.

Griffin E. A., Jr, Staknis D. and Weitz C. J. (1999) Light-independent role of CRY1 and CRY2 in the mammalian circadian clock. *Science* **286**, 768–771.

Guillaumond F., Dardente H., Giguère V. and Cermaian N. (2005) Differential control of Bmal1 circadian transcription by REV-ERB and ROR nuclear receptors. *J. Biol. Rhythms* **20**, 391–403.

Hasan S., van der Veen D. R., Winsky-Sommerer R., Hogben A., Laing E. E., Koentgen F., Dijk D. J. and Archer S. N. (2014) A human sleep homeostasis phenotype in mice expressing a primate-specific PER3 variable-number tandem-repeat coding region polymorphism. *FASEB J.* **28**, 2441–2454.

Hirano A., Yumimoto K., Tsunematsu R., Matsumoto M., Oyama M., Kozuka-Hata H., Nakagawa T., Lanjakornsiripan D., Nakayama K. I. and Fukada Y. (2013) FBXL21 regulates oscillation of the circadian clock through ubiquitination and stabilization of cryptochromes. *Cell* **152**, 1106–1118.

Jin X., Shearman L. P., Weaver D. R., Zylka M. J., de Vries G. J. and Reppert S. M. (1999) A molecular mechanism regulating rhythmic output from the suprachiasmatic circadian clock. *Cell* **96**, 57–68.

Kim T. D., Kim J. S., Kim J. H., Myung J., Chae H. D., Woo K. C., Jang S. K., Koh D. S. and Kim K. T. (2005) Rhythmic serotonin N-acetyltransferase mRNA degradation is essential for the maintenance of its circadian oscillation. *Mol. Cell. Biol.* **25**, 3232–3246.

Kim T. D., Woo K. C., Cho S., Ha D. C., Jang S. K. and Kim K. T. (2007) Rhythmic control of AANAT translation by hnRNP Q in circadian melatonin production. *Genes Dev.* **21**, 797–810.

Kim D. Y., Woo K. C., Lee K. H., Kim T. D. and Kim K. T. (2010) hnRNP Q and PTB modulate the circadian oscillation of mouse Rev-erb alpha via IRES-mediated translation. *Nucleic Acids Res.* **38**, 7068–7078.

Kim D. Y., Kwak E., Kim S. H., Lee K. H., Woo K. C. and Kim K. T. (2011) hnRNP Q mediates a phase-dependent translation-coupled mRNA decay of mouse Period3. *Nucleic Acids Res.* **39**, 8901–8914.

Kim D. Y., Kim W., Lee K. H., Kim S. H., Lee H. R., Kim H. J., Jung Y., Choi J. H. and Kim K. T. (2013) hnRNP Q regulates translation of p53 in normal and stress conditions. *Cell Death Differ.* **20**, 226–234.

Koike N., Yoo S. H., Huang H. C., Kumar V., Lee C., Kim T. K. and Takahashi J. S. (2012) Transcriptional architecture and chromatin landscape of the core circadian clock in mammals. *Science* **338**, 349–354.

Kojima S., Matsumoto K., Hirose M. *et al.* (2007) LARK activates posttranscriptional expression of an essential mammalian clock protein, PERIOD1. *Proc. Natl Acad. Sci. USA* **104**, 1859–1864.

Kojima S., Sher-Chen E. L. and Green C. B. (2012) Circadian control of mRNA polyadenylation dynamics regulates rhythmic protein expression. *Genes Dev.* **26**, 2724–2736.

Kume K., Zylka M. J., Shiram S., Shearman L. P., Weaver D. R., Jin X., Maywood E. S., Hastings M. H. and Reppert S. M. (1999) mCRY1 and mCRY2 are essential components of the negative limb of the circadian clock. *Cell* **98**, 193–205.

Kwak E., Kim T. D. and Kim K. T. (2006) Essential role of 3'-untranslated region-mediated mRNA decay in circadian oscillations of mouse Period3 mRNA. *J. Biol. Chem.* **281**, 19100–19106.

Lee H., Chen R., Lee Y., Yoo S. and Lee C. (2009) Essential roles of CKIdelta and CKIepsilon in the mammalian circadian clock. *Proc. Natl Acad. Sci. USA* **106**, 21359–21364.

Lee H. M., Chen R., Kim H., Etchegaray J. P., Weaver D. R. and Lee C. (2011a) The period of circadian oscillator is primarily determined by the balance between casein kinase 1 and protein phosphatase 1. *Proc. Natl Acad. Sci. USA* **108**, 16451–16456.

Lee K. H., Woo K. C., Kim D. Y., Kim T. D., Shin J., Park S. M., Jang S. K. and Kim K. T. (2011b) Rhythmic interaction between Period1 mRNA and hnRNP Q leads to circadian time-dependent translation. *Mol. Cell. Biol.* **32**, 717–728.

Lee K. H., Kim S. H., Lee H. R., Kim W., Kim D. Y., Shin J. C., Yoo S. H. and Kim K. T. (2013) MicroRNA-185 oscillation controls circadian amplitude of mouse Cryptochrome 1 via translational regulation. *Mol. Biol. Cell* **24**, 2248–2255.

Leloup J. C. and Goldbeter A. (2004) Modeling the mammalian circadian clock: sensitivity analysis and multiplicity of oscillatory mechanisms. *J. Theor. Biol.* **230**, 541–562.

Leloup J. C., Gonze D. and Goldbeter A. (1999) Limit cycle models for circadian rhythms based on transcriptional regulation in Drosophila and Neurospora. *J. Biol. Rhythms* **14**, 433–448.

Menet J. S., Rodriguez J., Abruzzi K. C. and Rosbash M. (2012) Nascent-Seq reveals novel features of mouse circadian transcriptional regulation. *Elife* **1**, e00011.

Morf J., Rey G., Schneider K., Stratmann M., Fujita J., Naef F. and Schibler U. (2012) Cold-inducible RNA-binding protein modulates circadian gene expression posttranscriptionally. *Science* **338**, 379–383.

Nakahata Y., Kaluzova M., Grimaldi B., Sahar S., Hirayama J., Chen D., Guarente L. P. and Sassone-Corsi P. (2008) The NAD+-dependent deacetylase SIRT1 modulates CLOCK-mediated chromatin remodeling and circadian clock. *Cell* **134**, 329–340.

Ohsaki K., Oishi K., Kozono Y., Nakayama K., Nakayama K. I. and Ishida N. (2008) The role of beta-TrCP1 and beta-TrCP2 in circadian rhythm generation by mediating degradation of clock protein PER2. *J. Biochem.* **144**, 609–618.

Parsons M. J., Leste K. J., Barclay N. L., Archer S. N., Nolan P. M., Eley T. C. and Gregory A. M. (2014) Polymorphisms in the circadian expressed genes PER3 and ARNTL2 are associated with diurnal preference and GNbeta3 with sleep measures. *J. Sleep Res.* **23**, 595–604.

Paulsen M. T., Veloso A., Prasad J., Bedi K., Ljungman E. A., Magnuson B., Wilson T. E. and Ljungman M. (2014) Use of Bru-Seq and BruChase-Seq for genome-wide assessment of the synthesis and stability of RNA. *Methods* **67**, 45–54.

Pendergast J. S., Niswender K. D. and Yamazaki S. (2012) Tissue-specific function of Period3 in circadian rhythmicity. *PLoS ONE* **7**, e30254.

Preitner N., Damiola F., Lopez-Molina L., Zakany J., Duboule D., Albrecht U. and Schibler U. (2002) The orphan nuclear receptor

REV-ERBalpha controls circadian transcription within the positive limb of the mammalian circadian oscillator. *Cell* **110**, 251–260.

Reppert S. M. and Weaver D. R. (2002) Coordination of circadian timing in mammals. *Nature* **418**, 935–941.

Sanchez S. E., Petrillo E., Beckwith E. J. *et al.* (2010) A Methyl transferase links the circadian clock to the regulation of alternative splicing. *Nature* **468**, 112–116.

Sangoram A. M., Saez L., Antoch M. P. *et al.* (1998) Mammalian circadian autoregulatory loop: a timeless ortholog and mPer1 interact and negatively regulate CLOCK-BMAL1-induced transcription. *Neuron* **21**, 1101–1113.

Schmal C., Reimann P. and Staiger D. (2013) A circadian clock-regulated toggle switch explains AtGRP7 and AtGRP8 oscillations in Arabidopsis thaliana. *PLoS Comput. Biol.* **9**, e1002986.

Schmutz I., Wendt S., Schnell A., Kramer A., Mansuy I. M. and Albrecht U. (2011) Protein phosphatase 1 (PP1) is a post-translational regulator of the mammalian circadian clock. *PLoS ONE* **6**, e21325.

Shirogane T., Jin J., Ang X. L. and Harper J. W. (2005) SCFbeta-TRCP controls clock-dependent transcription via casein kinase 1-dependent degradation of the mammalian period-1 (Per1) protein. *J. Biol. Chem.* **280**, 26863–26872.

Siepka S. M., Yoo S. H., Park J., Song W., Kumar V., Hu Y., Lee C. and Takahashi J. S. (2007) Circadian mutant Overtime reveals F-box protein FBXL3 regulation of cryptochrome and period gene expression. *Cell* **129**, 1011–1023.

Travnickova-Bendova Z., Cermakian N., Reppert S. M. and Sassone-Corsi P. (2002) Bimodal regulation of mPeriod promoters by CREB-dependent signaling and CLOCK/BMAL1 activity. *Proc. Natl Acad. Sci. USA* **99**, 7728–7733.

Ueda H. R., Chen W., Adachi A. *et al.* (2002) A transcription factor response element for gene expression during circadian night. *Nature* **418**, 534–539.

Wen F., Zhou R., Shen A., Choi A., Uribe D. and Shi J. (2012) The tumor suppressive role of eIF3f and its function in translation inhibition and rRNA degradation. *PLoS ONE* **7**, e34194.

Wilsbacher L. D., Yamazaki S., Herzog E. D., Song E. J., Radcliffe L. A., Abe M., Block G., Spitznagel E., Menaker M. and Takahashi J. S. (2002) Photic and circadian expression of luciferase in mPeriod1-luc transgenic mice invivo. *Proc. Natl Acad. Sci. USA* **99**, 489–494.

Woo K. C., Kim T. D., Lee K. H., Kim D. Y., Kim W., Lee K. Y. and Kim K. T. (2008) Mouse period2 mRNA circadian oscillation is modulated by PTB-mediated rhythmic mRNA degradation. *Nucleic Acids Res.* **37**, 26–37.

Woo K. C., Ha D. C., Lee K. H., Kim D. Y., Kim T. D. and Kim K. T. (2010) Circadian amplitude of cryptochrome 1 is modulated by mRNA stability regulation via cytoplasmic hnRNP D oscillation. *Mol. Cell. Biol.* **30**, 197–205.

Woo K. C., Kim T. D., Lee K. H. *et al.* (2011) Modulation of exosome-mediated mRNA turnover by interaction of GTP-binding protein 1 (GTPBP1) with its target mRNAs. *FASEB J.* **25**, 2757–2769.

Yoo S. H., Mohawk J. A., Siepka S. M. *et al.* (2013) Competing E3 ubiquitin ligases govern circadian periodicity by degradation of CRY in nucleus and cytoplasm. *Cell* **152**, 1091–1105.